GEOPHYSICS, VOL. 75, NO. 5 (SEPTEMBER-OCTOBER 2010); P. 75A67–75A81, 15 FIGS.
10.1190/1.3483451

Ten years of marine CSEM for hydrocarbon exploration

Steven Constable[1]

ABSTRACT

Marine controlled-source electromagnetic (CSEM) surveying has been in commercial use for predrill reservoir appraisal and hydrocarbon exploration for 10 years. Although a recent decrease has occurred in the number of surveys and publications associated with this technique, the method has become firmly established as an important geophysical tool in the offshore environment. This is a consequence of two important aspects associated with the physics of the method: First, it is sensitive to high electrical resistivity, which, although not an unambiguous indicator of hydrocarbons, is an important property of economically viable reservoirs. Second, although the method lacks the resolution of seismic wave propagation, it has a much better intrinsic resolution than potential-field methods such as gravity and magnetic surveying, which until now have been the primary nonseismic data sets used in offshore exploration. Although by many measures marine CSEM is still in its infancy, the reliability and noise floors of the instrument systems have improved significantly over the last decade, and interpretation methodology has progressed from simple anomaly detection to 3D anisotropic inversion of multicomponent data using some of the world's fastest supercomputers. Research directions presently include tackling the airwave problem in shallow water by applying time-domain methodology, continuous profiling tools, and the use of CSEM for reservoir monitoring during production.

INTRODUCTION

On 20 October 2000, the research vessel Charles Darwin sailed south from Tenerife to the Girassol prospect, Block 17, offshore Angola, to carry out the first survey of an oil field using marine controlled-source electromagnetic (CSEM) sounding (Ellingsrud et al., 2002). Just more than a year later, several more surveys were carried out in the same region (Constable and Srnka, 2007), and within two years of the first survey three contracting companies had been formed for the express purpose of providing commercial marine CSEM services to the exploration industry. Now, almost 10 years after the Girassol survey, marine CSEM is a broadly used, if not mainstream, geophysical technology, with over 500 surveys reportedly having been carried out and several custom-built survey vessels in operation. The 75th anniversary of GEOPHYSICS and the 10th anniversary of commercial marine CSEM seem to constitute an appropriate occasion to review the marine CSEM method: where we have been, where we are today, and where we might be going.

The aim of this paper is to provide a technical review, which is accessible to the nonexpert, of the marine CSEM method. However, to illustrate some of the important issues, original calculations have been made that, it is hoped, will be of interest to marine electromagnetic (EM) practitioners.

WHERE WE HAVE BEEN

The history of marine CSEM sounding is intimately linked to the history of the marine magnetotelluric (MT) method because both techniques aim to study seafloor resistivity and both rely on seafloor recordings of electric and magnetic fields. The difficulty associated with making actual seafloor measurements meant that theory significantly predated practice. In his seminal paper introducing the MT method for prospecting, Cagniard (1953) explicitly considered marine measurements but clearly did not appreciate the practical issues when he wrote, "there is no difficulty whatsoever in carrying out a correct galvanometric recording on board of a ship tossed about by the waves" (1953, p. 632). He was, however, mindful of the difficulty in making seafloor magnetic measurements and suggested using nearby land stations.

The corresponding first publication proposing marine CSEM measurements is probably that of Bannister (1968), who presented theory for frequency-domain, seafloor-to-seafloor dipole-dipole measurements to determine seabed resistivity. Bannister also recognized the noise problems associated with magnetometers vibrating or moving in earth's main field and recommended the horizontal electric dipole (HED) configuration that is used today. Other early papers of note include those of Brock-Nannestad (1965), who pro-

Manuscript received by the Editor 8 April 2010; revised manuscript received 1 June 2010; published online 14 September 2010.
[1]Scripps Institution of Oceanography, La Jolla, California, U.S.A. E-mail: sconstable@ucsd.edu.

posed a vertical gradient method similar to MT for the express purpose of estimating seafloor resistivity, and Coggon and Morrison (1970), who proposed a relatively high-frequency vertical magnetic dipole source for estimating shallow seafloor structure.

In the early 1960s, the team of Charles Cox and Jean Filloux developed the first equipment suitable for deep seafloor MT and CSEM soundings. In late 1961, Cox and Filloux had deployed both electric and magnetic field recorders in 1000- to 2000-m water offshore California, and in 1965 they deployed similar instruments in 4000-m water at a distance of 650 km from shore (Filloux, 1967b). The 1965 experiment did not produce simultaneous recordings of seafloor electric and magnetic fields, but by referencing both to land magnetic measurements a seafloor MT response was produced. The magnetometer that was used is described by Filloux (1967a).

A manuscript describing the electric field recorders, which consisted of 1-km-long seafloor cables connected to an amplifier and data logging system, appears to have been submitted to the *Journal of Marine Research* in 1966 but never published. The device is well documented in Filloux (1967b) and briefly noted by Cox et al. (1971), who also presented the MT data from the deep-seafloor site, and it appears again in Filloux (1973). Filloux (1974) went on to develop a more easily deployed electric field instrument incorporating a system for removing electrode offsets and drift by reversing the contact between a pair of electrodes and the pair of 3-m salt bridges that formed the antennas. This instrument was used extensively later for long-period, deep-seafloor MT sounding.

Cox (1980) proposed the use of HED controlled-source sounding to study seafloor geology. With characteristic insight, Cox noted that the method would be most suitable for studying resistive layers, and that "the most effective mode propagating from a horizontal electric dipole is TM: the electric field is nearly vertical in the poorly conducting rocks" (1980, p. 154). As we will discuss below, it is the transverse magnetic (TM), or radial, mode that is used for hydrocarbon exploration. Cox (1981) expanded on the concept of marine CSEM and described a deep-sea experiment he had carried out in 1979. A manuscript describing the equipment (Cox et al., 1981) was submitted to *Radio Science* in 1981 but, again, not published at that time. It appears that Cox was not aware of the Bannister paper and proposed the method independently.

Although steady academic activity in marine EM has occurred since the 1970s (see the reviews by Constable, 1990; Palshin, 1996; and Baba, 2005), it is only in the last decade that the use of marine

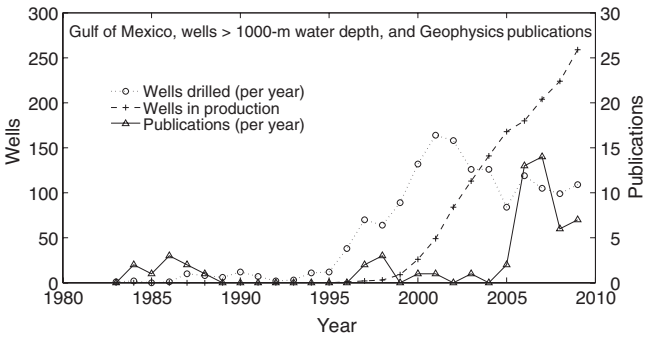

Figure 1. The number of Gulf of Mexico wells in water depths greater than 1000 m, drilled and in production, and the number of publications related to marine EM published in GEOPHYSICS since 1980.

CSEM and MT for exploration has been significant. Marine CSEM sounding and marine MT sounding were developed as academic tools to study the oceanic lithosphere and mantle. Although the potential to use marine CSEM in the exploration environment was recognized quite early (Constable et al., 1986; Srnka, 1986; Chave et al., 1991), it was not until exploration moved into deep water that industry developed a strong interest in marine EM methods. This is illustrated in Figure 1, which shows the number of wells drilled, and the number of wells in production, at water depths greater than 1000 m in the Gulf of Mexico (compiled using data from Minerals Management Service, 2010). It can be seen that exploration at these depths started in the late 1990s, and that production started only in the early 21st century, as tension-leg platforms and other deepwater technologies were developed.

Ironically, it was marine MT, initially thought to be of little use in the offshore exploration environment (see Chave et al., 1991), that was first commercialized for use on the continental shelves (Constable et al., 1998; Hoversten et al., 1998) as a tool for mapping geology in areas where seismic methods produced poor results (salt, basalt, and carbonate provinces). At this time, marine MT was viewed as a deepwater exploration tool whose use was justified by the high cost of drilling. Although only a half-dozen commercial marine MT surveys were carried out in the five years prior to 2000, the establishment of MT field crews and equipment facilitated early progress in CSEM because the receiver equipment is essentially the same for both marine EM methods. The marine CSEM method operates best in deep water (more so than MT), and the rise in CSEM exploration coincides with the ability to produce hydrocarbons in water depths greater than 1000 m. The high cost of deepwater drilling also supported the use of a relatively expensive nonseismic method.

The former Soviet Union was an early adopter of electromagnetic methods for oil and gas exploration on land, and there was certainly Soviet interest in marine MT exploration, but early work consisted mainly of magnetovariational and gradient studies or towed electrokinetograph measurements (Fonarev, 1982). Trofimov et al. (1973) report MT results collected on floating ice in the Arctic Ocean. In spite of the interest in CSEM as an exploration tool on land, there seems to have been no migration into the ocean; according to Belash, "Marine electromagnetic probing is not conducted at present on account of an inadequate theoretical background" (1981, p. 860).

Figure 1 also shows the number of publications in GEOPHYSICS dealing with the broad subject of marine EM, which we might use as a measure of exploration interest in this field. Prior to 1984, no references exist except the Bannister (1968), Filloux (1967a), and Coggon and Morrison (1970) papers cited above. All nine publications between 1984 and 1998 are written by Nigel Edwards or his students, either on model studies of time-domain EM (e.g., Edwards et al., 1984; Edwards and Chave, 1986; Cheesman et al., 1987; Edwards, 1997) or on the application of magnetometric resistivity to the marine environment (e.g., Edwards et al., 1985; Wolfgram et al., 1986). The next three publications all deal with the commercial application of marine MT (Constable et al., 1998; Hoversten et al., 1998; Hoversten et al., 2000). Thirty-four papers published in GEOPHYSICS since then deal with marine CSEM; probably a similar number of articles appear in the other relevant journals.

It can be seen from Figure 1 that although exploration CSEM started in 2000, the large jump in publications came in 2006. This jump is partly associated with the gestation time for refereed publi-

cations, but it occurred also because truly independent commercial activity did not start until about 2004. Prior to that, surveys were being carried out with academically built instruments, mostly receivers made by Scripps Institution of Oceanography and transmitters made by Southampton University. Constable and Srnka (2007) describe much of this early development, but Figure 2 serves to show how rapid progress was made by the efforts of two oil companies, two academic institutions, and a small MT contractor. The importance of marine CSEM and the contributions made by this small group's early work were recognized in the SEG 2007 Distinguished Achievement Award.

Figure 1 suggests a recent downturn in marine CSEM publications. This is largely an artifact of the 2007 GEOPHYSICS special issue on the subject, but is in fact coincident with a decrease in commercial activity. This decrease can be interpreted as a natural decay to an equilibrium demand after an initial and enthusiastic rush to gain some experience with a new technology, perhaps exacerbated by the economic downturn. The longer-term concern is that interpretation tools, particularly those that integrate CSEM results with other geophysical and geologic data, have lagged behind the data acquisition capabilities, and thus companies that have commissioned marine CSEM surveys, or are partners of companies that have, cannot always make the best use of the data. Acceptance of marine EM techniques will be complete only when the larger client companies have the in-house software needed to invert EM data and incorporate the resulting models into integrated exploration programs, and the smaller companies can obtain the same services from independent consultants.

A SIMPLE OVERVIEW OF THE METHOD

Figure 3 illustrates the marine CSEM method. Electric and magnetic field recorders are deployed on the seafloor, weighed down by environmentally benign anchors made from standard or degradable concrete. Electromagnetic fields are broadcast from a horizontal antenna, 50 to 300 m long and emitting as much as a thousand amps of current into the seawater. The transmitter and antenna are towed close to the seafloor (commonly at a height of 25 to 100 m) to maximize coupling with seafloor rocks and sediments and to minimize coupling with the air. Transmission currents are typically binary waveforms with 0.1- to 0.25-Hz fundamental and higher harmonics. Square waves, with geometrically decreasing odd harmonics, were used initially (e.g., Ellingsrud et al., 2002), although the present trend is to shape the waveform to have a more desirable frequency content (e.g., Mittet and Schaug-Pettersen, 2008; Constable et al., 2009); a similar approach was used early on for academic surveys by Cox et al. (1986) and Constable and Cox (1996).

Considerable confusion often exists when trying to explain the inherent resolution of marine CSEM and MT to nonpractitioners, and thus it is useful to relate these methods to the more familiar seismic and potential-field (gravity, magnetics, and DC resistivity) techniques. We start with the damped wave equation used to describe the vector electric field **E** in ground-penetrating radar:

$$\nabla^2\mathbf{E} = \mu\sigma\frac{\partial\mathbf{E}}{\partial t} + \mu\epsilon\frac{\partial^2\mathbf{E}}{\partial t^2}, \quad (1)$$

where t is time, σ is conductivity (between 10^0 and 10^{-6} S/m in typical rocks), μ is magnetic permeability (usually taken to be the free space value of $4\pi\times10^{-7}$ H/m in rocks lacking a large magnetite content), and ϵ is electric permittivity (between 10^{-9} and 10^{-11} F/m, depending on water content). The first term (in σ) is the loss term, and disappears in free space and the atmosphere where $\sigma \approx 0$, leaving the lossless wave equation that will be familiar to seismologists. The vertical resolution of wave propagation is proportional to inverse wavelength, and a wave carries information accumulated along its entire raypath. Thus, as long as geometric spreading and attenuation do not prevent detection, a seismic wave carries similar resolution at depth as it does near the surface.

However, in rocks where σ is typically 10^9 times bigger than ϵ, the loss term dominates until the frequency is high enough for the second derivative term to be significant. For ground-penetrating radar, operating at a frequency of about 100 MHz, the second term is large enough to provide wave propagation, although the loss term still prevents penetration of more than a few tens of meters even in relatively resistive ground. At frequencies relevant to marine CSEM (from 0.1 to 10 Hz) and MT (from 0.0001 to 1 Hz), the second de-

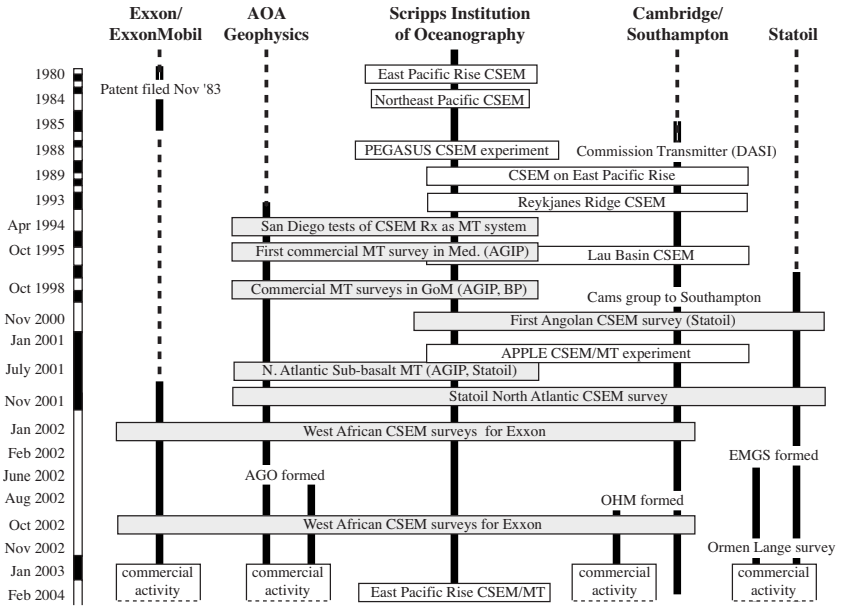

Figure 2. A timeline for the early development of commercial marine EM (nonlinear scale). Between 1989 and 2001, academic experiments (white boxes) were collaborations between Scripps Institution of Oceanography (SIO) and Cambridge University (later Southampton), which was the model for the first Angolan oil-field survey commissioned by Statoil in 2000 as well as several subsequent surveys for ExxonMobil and Statoil. AOA Geophysics developed a commercial marine MT capability in 1995 and was involved in early Statoil and ExxonMobil surveys until spinning off AOA Geomarine Operations (AGO) in 2002, the same year that Southampton University formed Offshore Hydrocarbon Mapping (OHM) and Statoil formed Electromagnetic Geoservices (EMGS). Within a few years, EMGS, OHM, and AGO were all carrying out independent commercial surveys, although AGO and OHM continued to combine efforts for several years to field transmitters and receivers. In the last few years, several other companies have started offering marine CSEM services in addition to the original three.

rivative term is negligibly small and the damped wave equation reduces to a diffusion equation:

$$\nabla^2\mathbf{E} = \mu\sigma\frac{\partial\mathbf{E}}{\partial t}, \tag{2}$$

which for a uniform harmonic excitation at angular frequency ω has solutions of the form

$$\mathbf{E} = \mathbf{E}_o e^{-i\beta z} e^{-\alpha z}, \tag{3}$$

where α and β are exponential attenuation and phase lag terms over distance z, related to the well-known skin depth z_s:

$$z_s = 1/\alpha = 1/\beta = \sqrt{2/(\sigma\mu_o\omega)}. \tag{4}$$

The skin depth is the distance over which field amplitudes are reduced to $1/e$ in a uniform conductor, or about 37% (given by α), and the phase progresses one radian, or about 57° (given by β). Skin depth is fairly well approximated by

$$z_s \approx \frac{500 \text{ meters}}{\sqrt{\sigma f}}, \tag{5}$$

where ordinary frequency $f = \omega/(2\pi)$.

Unlike heat flow, for EM induction the frequency of the forcing function is under the control of the geophysicist and provides an intrinsic sensitivity to depth. However, when one progresses from the wave equation to the diffusion equation, the concept of resolution changes drastically. For a harmonic excitation, the entire earth/sea/air system is excited by EM energy, and what is measured at the receiver is a kind of average of the whole system weighted by the sensitivity to each part of the system, which decreases with increasing distance from the observer. Thus a 1-m object is easy to detect when buried 1 m below the seafloor, but impossible to see when buried 1000 m deep. Attempts to mimic seismic methods by creating an impulsive source (essentially what is done in the time-domain EM, or TEM, method) does not avoid the loss of resolution because skin-depth attenuation ensures that the pulse broadens as it propagates into the ground and the sensitivity kernels again decrease with depth. These concepts should become clearer as we discuss issues of sensitivity and TEM methods below.

One often is asked to quantify the resolution of inductive EM methods, and 5% of the depth of burial seems to be a reasonable estimate for both lateral and vertical resolution when EM data are interpreted on their own. (We will also see below that obtaining CSEM data accurate to better than 5% is difficult given the current navigation tools.) Simple model studies suggest one might do better, but simple model studies invariably neglect variations in the conductivity and anisotropy of the host rocks, and often include hidden assumptions or additional information. For example, layered models might be used to generate the model data, and then the solution space restricted to layered models during inversion (which tends to give good results). The corollary is that the incorporation of additional information into the interpretation of marine EM data can improve resolution significantly.

Although going from the wave equation to the diffusion equation represents a substantial loss of resolution, things can get worse. When the frequency goes to zero, equation 2 reduces to the Laplace equation

$$\nabla^2\mathbf{E} = 0, \tag{6}$$

which describes potential-field methods, and intrinsic resolution becomes almost nonexistent. Any surface gravity map can be explained by an arbitrarily thin surface layer of variable density, and any DC resisistivity sounding can (at least in one dimension) be explained by an arbitrarily thin surface layer of variable conductivity. Although bounds on deepest depth can be derived, and valuable information can be provided when independent information on depth and structure is available (e.g., from seismic data, geologic mapping, or well logs), potential-field methods have little resolution on their own.

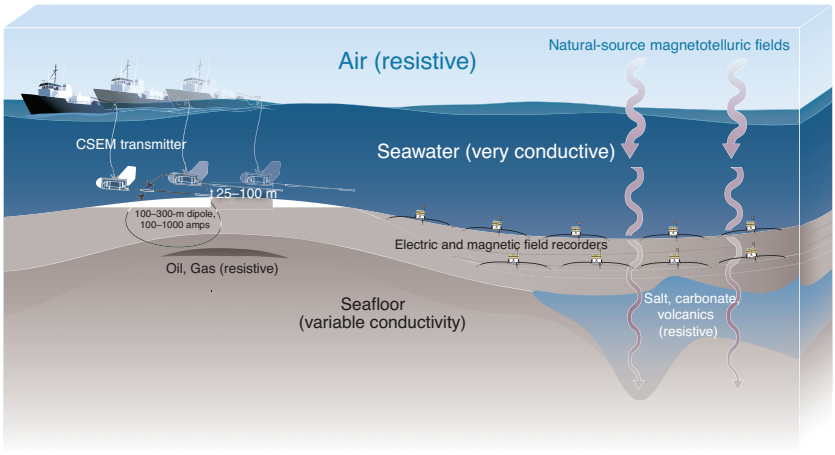

Figure 3. Marine EM concepts: Electric and magnetic field receivers are deployed on the seafloor to record time-series measurements of the fields, which could be used to compute MT impedances. The seafloor instruments also receive signals emitted by a CSEM transmitter (towed close to the seafloor) at ranges of as much as about 10 km. The MT signals are associated with largely horizontal current flow in the seafloor, and are sensitive only to large-scale structure. The CSEM signals involve both vertical and horizontal current flow, which could be interrupted by oil or gas reservoirs to provide sensitivity to these geologic structures even when they are quite thin.

Thus we see that inductive EM methods such as CSEM and MT sounding will never have the resolution of the seismic method, but they have much better resolution than potential-field methods. In particular, the ability to sample different frequencies provides an ability to control the depth of sensitivity. Of course, one can use the complete equation 1 to interpret CSEM data (e.g., Løseth et al., 2006), but that by itself will not change the resolution of the method. One can also note that equations 3 and 4 imply an apparent phase velocity that will be proportional to conductivity (and frequency), but again, this is not associated with wave propagation in the usual sense.

If no seismic signature is associated with a geologic target (say, an oil-water contact), then the superior resolution of the seismic method is of no help. In practice, it is the opposite problem, too large a seismic signature, which is more of a limitation. The use of marine MT was motivated by the large acoustic contrasts between sediments and rocks such as evaporites, carbonates, and volcanics, all of which are coincidentally resistive. Although acoustic reverberations and reflections

make it difficult to image beneath the upper surfaces of these lithologies, they might be broadly mapped using marine MT.

The use of marine CSEM has been motivated by the particular sensitivity of seismic methods to trace amounts of gas in the pore fluid ("fizz-gas"). Figure 4 illustrates the problem. Although small fractions of gas in pore fluid changes seismic velocity by almost a factor of 2, significant changes in resistivity are not achieved until the pore fluid is dominantly gas. The most extensive application of marine CSEM to date has been predrill appraisal of seismically identified direct hydrocarbon indicators, to avoid drilling dry holes associated with structures that are characterized by strong seismic reflections but are conductive.

Another difficulty in understanding EM methods is that several mechanisms are at work to produce changes in amplitude and phase (Figure 5). The first is geometric spreading from the transmitter, which in the low-frequency limit is simply the characteristic $1/(range)^3$ dipole decay that is familiar to users of DC resistivity sounding. The second is the galvanic effect associated with current passing across a conductivity boundary. The normal component of current must be continuous (from conservation of charge), and so Ohm's law ($\mathbf{J} = \sigma\mathbf{E}$, where $\mathbf{J}$ is current density) requires a jump in the electric field. Again, this is low-frequency behavior characteristic of DC resistivity sounding and, like the geometric effects, has no associated change in phase. Finally, the process of inductive attenuation and phase shift occurs when the skin depths are comparable to the distance over which the EM energy has traveled.

THE THIN RESISTIVE LAYER REVISITED

We can put these concepts together to help understand the sensitivity of the CSEM method to hydrocarbon reservoirs (Figure 6). In the direction inline with the transmitter dipole antenna, electric field lines are purely radial and plunge into the seafloor with a significant vertical component. The associated currents can be interrupted by tabular resistors such as reservoirs, producing a galvanic distortion of the electric field. This will be visible on the seafloor as increased electric field amplitude. In the direction broadside to the transmitter, electric fields are purely azimuthal and largely horizontal, and will not produce a galvanic response to horizontal boundaries. This results in a large difference in sensitivity between the radial and azimuthal geometries to thin resistive layers. This result was noted in a 1984 proposal submitted to 14 oil companies by Scripps; the authors examined a buried resistive layer model and concluded, "It is the TM mode of the experiment which is most sensitive to resistive structure. This makes the choice of transmitter geometry most important" (Cox et al., 1984, appendix 1, p. 3).

Unfortunately, the idea of using marine CSEM to explore for oil was 15 years ahead of its time, and it was not until Eidesmo et al. (2002) noted the same effect that this became the common knowledge it is today. Figure 7 shows the now-familiar CSEM response of

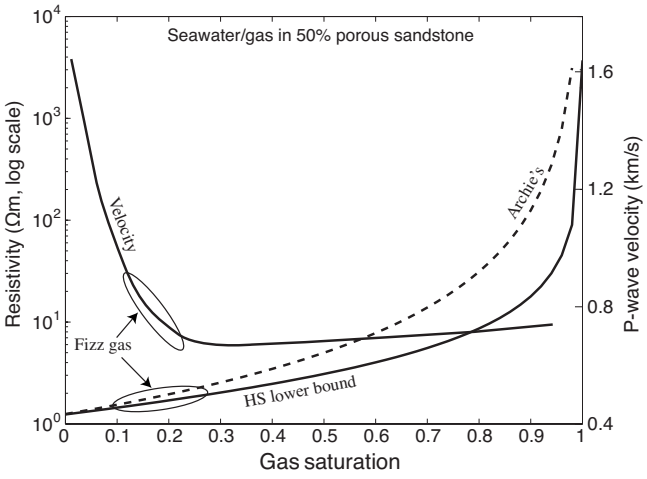

Figure 4. Seismic P-wave velocity (from Lee, 2004) and electrical resistivity of a porous (50%) sandstone as a function of gas saturation in the pore fluid. The largest effect on acoustic velocity occurs for the first few percent of gas fraction, but disconnected bubbles have little effect on resistivity, which does not increase significantly until gas saturations of 70% to 80% are achieved. The Hashin-Shtrikman (HS) bound is probably the most reasonable mixing law for the resistivity of gas bubbles in water, but Archie's law is provided for reference.

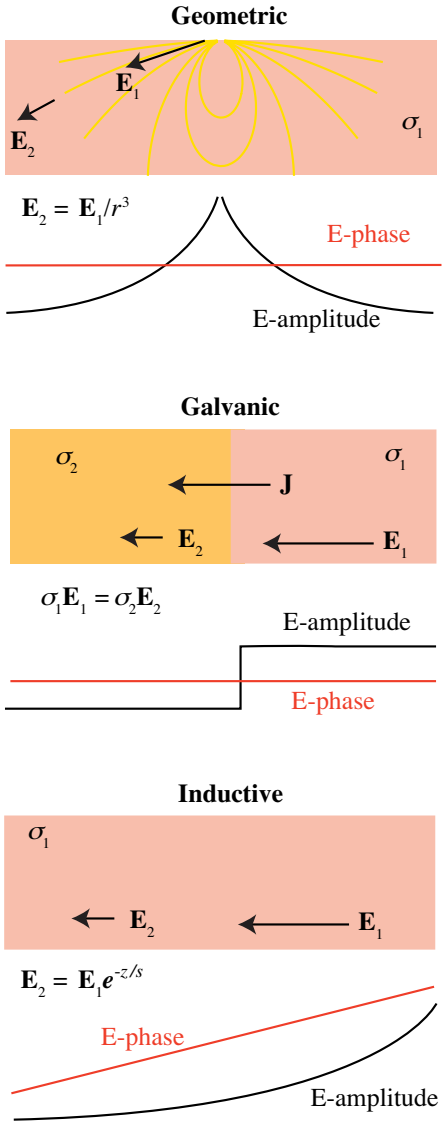

Figure 5. Three mechanisms are at work determining the amplitude and phase of CSEM signals as a function of source–receiver offset. The first is simple geometric spreading from a dipole, the second is a galvanic change in the electric field as current crosses a conductivity boundary, and the third is inductive attenuation. Only induction produces a change in phase.

the 1D canonical oil-field model, a 100-m/100-Ωm reservoir buried 1000 m deep in 1-Ωm sediments, in 1000-m water depth (inspired by the Girassol prospect). One sees a factor of 10 difference in the radial field amplitudes, which is largely a galvanic effect, and barely a factor of 2 in the azimuthal mode, which is mostly inductive.

Eidesmo et al. (2002) also noted that a buried thick layer of intermediate resistivity could mimic the radial mode amplitudes of an oil-field model (Figure 8), and that azimuthal mode data were needed to avoid confusion between the two models. Azimuthal data are, however, costly to collect compared with radial mode data. If receivers are deployed in a line on the seafloor and the transmitter towed along them, then a dense amount of purely radial mode data is collected. To collect coincident azimuthal mode data requires many crossing tows, with only one data point per instrument at each crossing, or a full 3D survey obtained by deploying a grid of receivers and towing a grid of transmitter lines. However, the two models are distinguished clearly by examining the radial mode phase (Figure 8c).

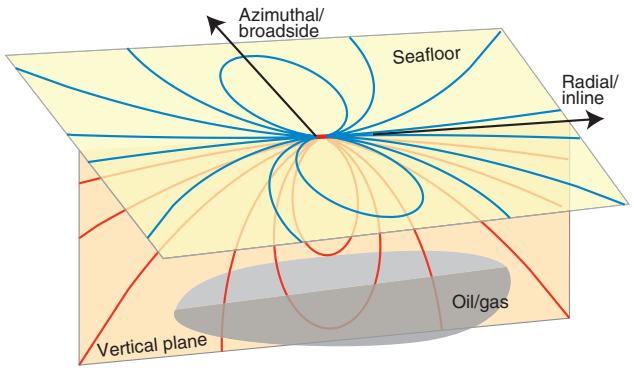

Figure 6. The dipole geometry of a near-seafloor transmitter. The maximum vertical electric fields (red) are below the transmitter in the inline direction. Here fields are of purely radial geometry and able to generate galvanic effects when they intersect subhorizontal, tabular bodies such as oil and gas reservoirs. In the broadside direction, electric fields are purely azimuthal and largely horizontal, producing little interaction with the reservoir.

This is understood easily in terms of the inductive and galvanic effects described above. The increased amplitudes (compared with the half-space model of Figure 7) from the oil-field model are a result of galvanic effects. The increased amplitude of the confounding thick-layer model is a result of larger skin depths, which will be associated with smaller phase lags (compared with the 1-Ωm oil-field host sediments). As predicted, the phase lag of the confounding model is 50° less at a range of 3 km. Because the confounding model is produced by balancing galvanic effects with skin depth, the equivalence in radial mode amplitude also disappears if a different frequency is considered, illustrated by the 1-Hz radial mode responses shown in the figure.

If the sensitivity of CSEM to thin resistive layers is a galvanic effect similar to DC resistivity, then one might expect the transverse resistance (T)-equivalence one sees in DC resistivity sounding to hold. In other words, the transverse resistance $T = \rho t$, the product of a layer's resistivity ρ and thickness t, determines the response, and one cannot identify ρ and t independently of each other. Figure 9 shows that this is indeed the case, at least at relatively low frequencies (here, 0.1 Hz). The radial mode data for the two models are identical, even though the thick version of the layer is buried only at a depth of twice its thickness. The azimuthal mode has a small (15%) difference in response because it is primarily sensitive to both layers through induction, instead of a galvanic response. The inductive response can be increased by increasing frequency, and at 3 Hz both modes have a 60% difference in response to the two models, although this occurs close to the noise floor of the method (about 10^{-15} V/Am^2).

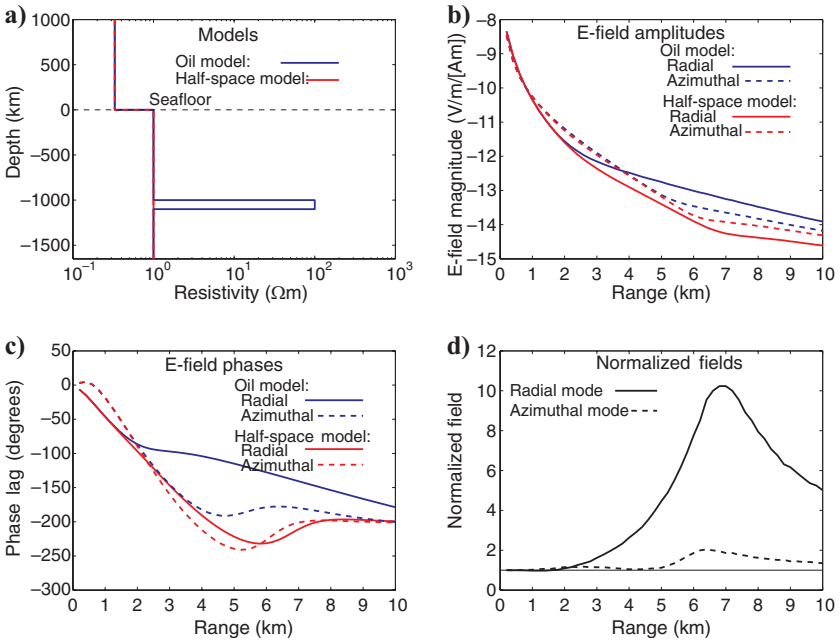

Figure 7. The radial and azimuthal CSEM responses of (a) the canonical oil-field model (blue) compared with a half-space (red), at a frequency of 0.25 Hz. The (b) amplitudes show a bigger response in the radial mode (solid lines) than in the azimuthal mode (broken lines). A similar behavior is seen in (c) the phase. In (d), we have plotted the radial and azimuthal oil-model amplitudes normalized by the half-space values.

Constable and Weiss (2006) show that for reservoirs of limited lateral extent, if the source and receiver are above the reservoir and within the lateral limits of the structure, the 3D response is well approximated by the type of 1D modeling we present here. They also show that when the lateral extent is less than twice the depth of burial, it becomes difficult to resolve the existence of the feature.

Using a series of inversions of synthetic 1D data, Key (2009) demonstrates that inverting two well-spaced frequencies (about a decade apart) of CSEM amplitudes and phases produces much better sensitivity to thin resistive targets than inverting single frequencies, but that adding additional frequencies does not improve resolution. Key also shows that inverting radial electric field data from a horizontal electric transmitter is as good as, or better than, inverting any other combination of source and receiver (i.e., azimuthal electric, vertical electric, horizontal magnetic), and that even inverting a combination of geometries does not improve resolution significantly, at least in one dimension. One does as well inverting the magnetic field in the radial direction (but which is crossline in orientation) as inverting the radial electric field, but magnetic field sensors are very much more sensitive to motion of the receiv-

er instrument, which favored the use of electric fields during the early academic applications of marine CSEM. However, the development of instruments stable enough to make good MT measurements on the continental shelf allowed magnetic field CSEM data to be collected with comparable noise floors to electric field data. Figure 10 shows a comparison of magnetic and electric field amplitude data over the Scarborough gas field offshore Western Australia (Myer et al., 2010).

MODELING

A frequency-domain 1D solution for a horizontal electric dipole transmitter has been available since Chave and Cox (1982) published their analysis of the 1D method. Flosadottir and Constable (1996) made some changes to the Chave and Cox forward code and implemented the regularized Occam's inversion scheme of Constable et al. (1987). Since then, several other codes have been written, such as the fully anisotropic model of Løseth and Ursin (2007) and the code of Key (2009) mentioned above. The Key code allows any source — receiver geometry and component, includes the Occam's inversion scheme, and is publicly available.

The relative speed and simplicity of 1D modeling has made it an attractive tool for CSEM interpretation, particularly because, as noted above, the 1D approximation is quite good for tabular bodies when both source and receiver are over the target. Of course, there will be limitations to using 1D interpretation over more complicated features. Perhaps more importantly than the dimensionality of the target, interpreting CSEM data a single receiver at a time (or a single midpoint gather) limits the amount of signal to noise available to resolve a given structure. The synthetic studies of Key (2009), as well as some recent work on the real data shown in Figure 10 (Myer et al., 2010), suggest that even though there might be a significant response from the target structure in the data, to resolve the difference between the thin resistor response of a reservoir and a broader background increase in resistivity requires fitting radial mode data to about 1%. Again, Figure 8 shows the similarity in the amplitude response for the two structures — inversion will rely heavily on the frequency dependence of the complex response of the radial field (i.e., fitting both amplitude and phase), or adding other information such as MT or the azimuthal CSEM response (Constable and Weiss, 2006).

Drawing from experience in MT modeling, the benefit of graduating from 1D inversion to 2D inversion is much greater than getting the dimensionality of the target correct, but it includes the benefit of applying the combined resolving power of many sites to a single model. For example, the individual MT responses inverted in two dimensions by Key et al. (2006) are almost one-dimensional in appearance, and exhibit only a very small signal from the salt body of interest (which, being a discrete resistor in a conductive host, is a difficult target for MT). However, when many sites are inverted in two dimensions, the combined data set does a reasonable

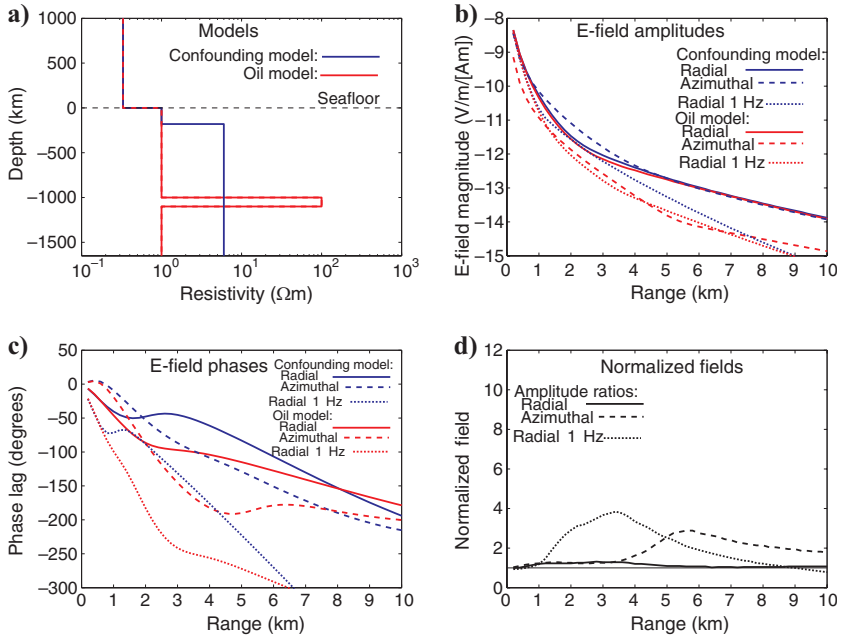

Figure 8. The radial and azimuthal CSEM responses of (a) the canonical oil-field model (red) compared with (b) a thick layer of intermediate resistivity (blue), at a frequency of 0.25 and 1 Hz (radial mode only). The (b) 0.25-Hz radial mode amplitudes are almost the same for the two models, whereas the azimuthal amplitudes are not, as noted by Eidesmo et al. (2002) and evident in (d) the ratio plot. However, (c) the 0.25-Hz radial mode phases are quite distinct for the two models, as are the 1-Hz radial mode amplitudes.

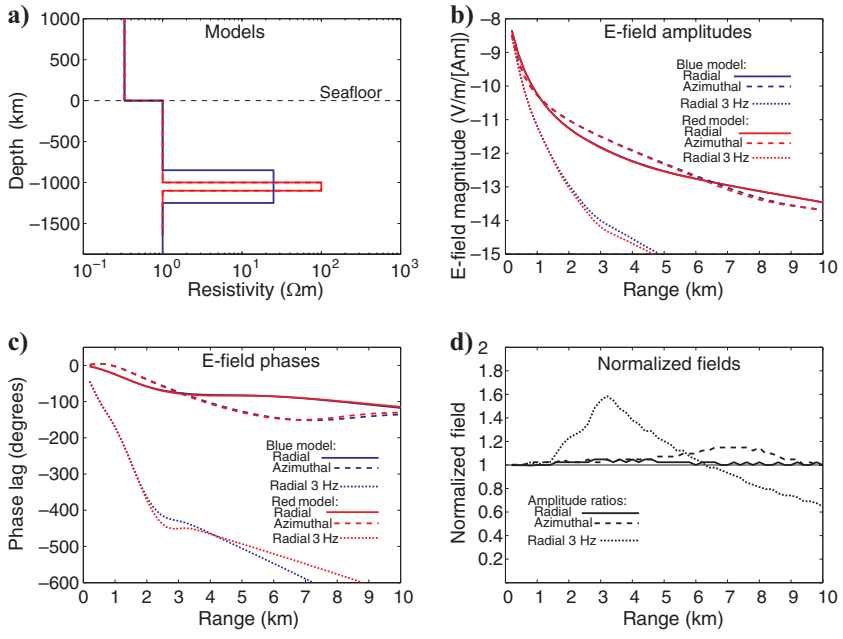

Figure 9. The CSEM responses at a frequency of 0.1 Hz for two T-equivalent models, one 100 m thick and one 400 m thick, as well as 3-Hz radial mode responses. The 0.1-Hz radial mode responses are almost identical, although there is a small azimuthal mode response. The 3-Hz data, however, can distinguish the two models, although the signal is close to the noise floor.

job of resolving the salt, and one might expect similar behavior for CSEM.

Because of the 3D nature of the source field, the move from one to two dimensions for CSEM modeling is not as easy as it is for MT modeling. (Some authors use the term 2.5D to describe 2D modeling with a 3D source field — this seems unnecessary and inconsistent with the use of one dimension to describe 1D CSEM modeling.) Indeed, from an algorithmic point of view, in marine CSEM it is easier to go directly to three dimensions and avoid the complexity of collapsing the along-strike fields in 2D models using a transformation, and this is what industry has tended to do. Finite-difference algorithms, in which the differential form of Maxwell's equations are approximated by differencing fields between nodes on an orthogonal mesh, have proved particularly attractive for 3D CSEM modeling, and several codes have been written (e.g., Newman and Alumbaugh, 1997; Weiss and Constable, 2006; Commer and Newman, 2008). One disadvantage of finite-difference meshes is that small node spacings, perhaps necessary to capture and accurately model structure in one part of the mesh, propagate in all three directions, making the mesh very large. However, 3D forward modeling using this scheme is quite tractable on modern computers. When one requires inversion, on the other hand, the computational requirements become significant (e.g., Commer et al., 2008).

A practical 2D marine CSEM inversion using the finite-element algorithm, in which EM fields are described by analytically differentiable basis functions across triangular elements, was written some time ago (Unsworth and Oldenburg, 1995) and used on practical data

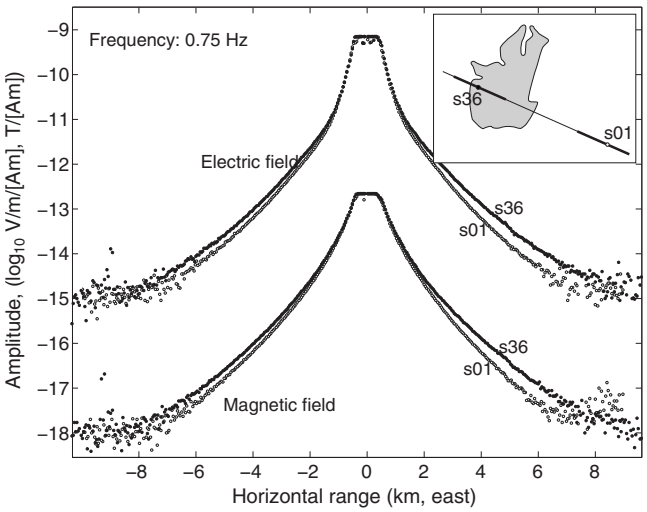

Figure 10. One-minute stacks of inline CSEM amplitude data on and off an Australian gas field, outlined in the inset. Site s01 (open circles) is well off the target structure, and site s36 (filled circles) is positioned over the west edge of the target. Noise floors for the electric and magnetic fields are approximately 10^{-15} V/Am^2 and 10^{-18} T/Am, respectively, limited in this case by environmental noise associated with tidal water currents. The electric field data have a very slight advantage in terms of maximum source–receiver range for a given signal-to-noise ratio. There is a factor of 2 enhancement of field amplitudes when source and receiver s36 are both over the reservoir (positive ranges) and slightly less when only the receiver is over the target (negative ranges). The target is about 1000 m below seafloor. From Constable et al. (2009).

by MacGregor et al. (2001), but the code was never distributed widely and has not seen broad application, although proprietary versions are probably in use today. A finite-element forward code for CSEM was written by Li and Key (2007) and has been broadly distributed. A 2D finite-difference forward and inverse code was published by Abubakar et al. (2008) and used on real data (K. Weitemeyer, G. Gao, S. Constable, and D. Alumbaugh, personal communication, 2010), but this code is proprietary. Other 1D, 2D, and 3D codes have been written and are being used on a proprietary basis also. Proprietary restrictions on access make it difficult to validate and compare codes, and the author has seen examples of very different results being obtained from the same data set by different contractors using different inversion codes. One interesting aspect of the Weitemeyer et al. study (K. Weitemeyer, G. Gao, S. Constable, and D. Alumbaugh, personal communication, 2010) is that the forward computations of the finite-difference code used in the inversion were compared to calculations made using the finite-element code of Li and Key (2007) to ensure that the finite-difference mesh was fine enough to be accurate.

Given the great computational cost of 3D inversion, the fact that most marine CSEM data are collected as individual lines of radial-component data (or a small number of parallel or intersecting lines), and the observation that 2D inversion has become an effective workhorse for MT interpretation even as 3D inversion has become tractable, one could ask what the relative gains of 3D inversion might be. Certainly, a few spectacular examples of 3D CSEM inversion have been shown at meetings (e.g., Carazzone et al., 2008; Price et al., 2008), and eventually appropriate comparisons of 2D and 3D inversions of synthetic and real data will be carried out and published. Meanwhile, we can examine the morphology of the resolution kernels for marine CSEM to get some understanding of this issue.

In Figure 11, we plot a discrete version of the resolution kernels for the radial electric field and the inline magnetic field for a 1-Ωm half-space. The figures were made using the 3D finite-difference code of Weiss and Constable (2006) and by individually perturbing each $400 \times 400 \times 200$-m element of the finite-difference grid. These figures illustrate that the marine CSEM method is primarily sensitive to structure beneath and between the transmitter and receiver, and that changes in conductivity more than about half the source-receiver spacing in the crossline or vertical direction have little effect on the data. Thus one might expect that for a single line of receivers with a transmitter line towed along it, 2D interpretation will be effective and accurate. Of course, a half-space represents an end-member model, and resistive structure near the transmitter or receiver will couple into the CSEM fields to some extent and extend the region over which fields are sensitive to structure. However, most of the seafloor relevant to exploration has fairly uniform conductivity in the shallow parts of the section, and exceptions to this are likely to be obvious in the data.

The concept demonstrated here is that 2D modeling and inversion of single lines of CSEM data constitute a reasonable approach to data interpretation, but this demonstration does not address the need to collect 3D data sets. Indeed, a corollary of this analysis is that offline structure will easily be missed by a single line of data, and thus depending on the goals of the survey one might need to collect 3D data, several lines of 2D data, or at least data from offline transmitter tows. In addition, as we discuss below, if one needs to resolve anisotropy, azimuthal mode data will need to be collected along with the radial mode data obtained from single lines.

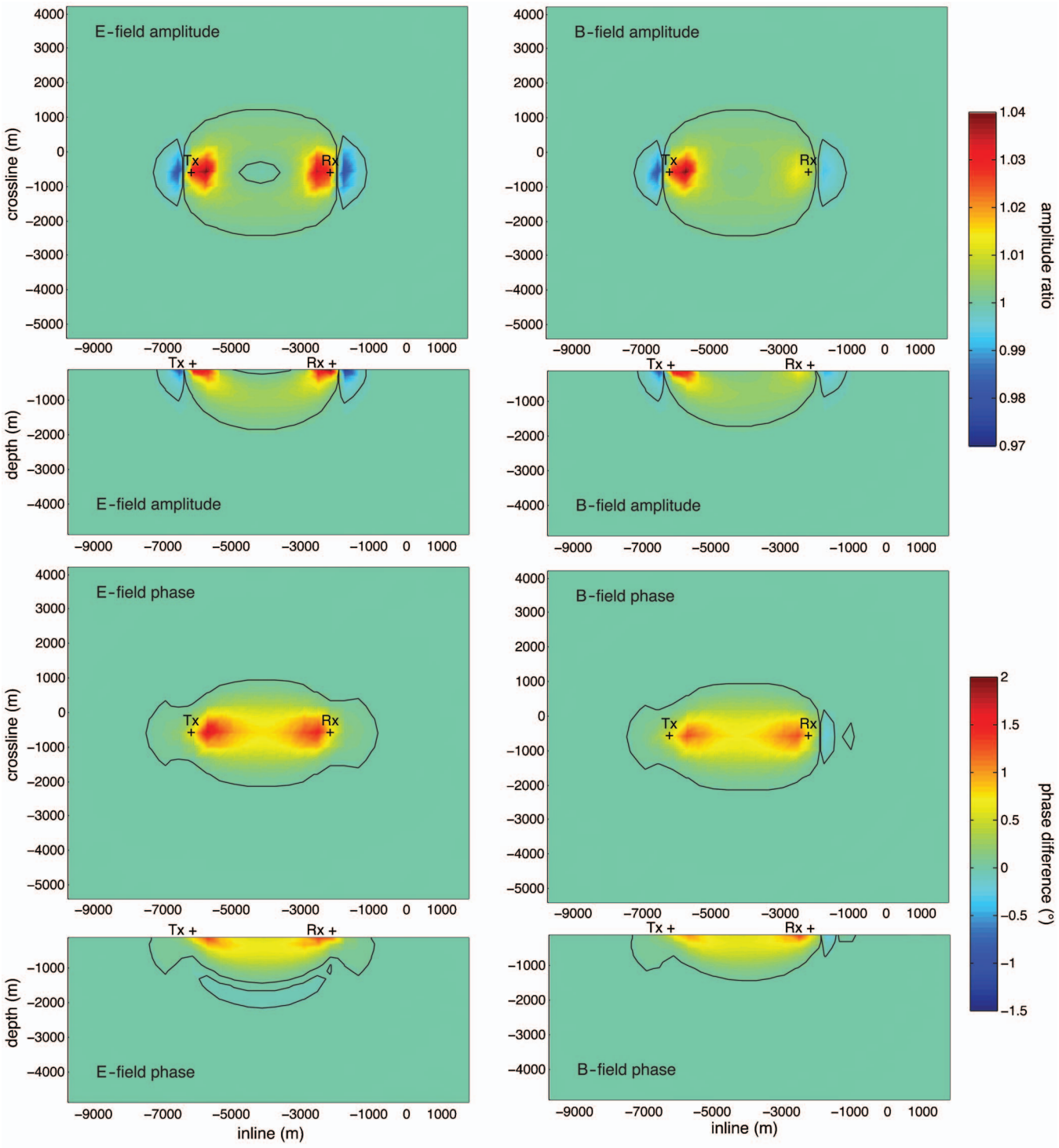

Figure 11. Sensitivity of the marine CSEM method to a 1-Ωm seafloor. Computations are made with the code of Weiss and Constable (2006) with a finite-difference mesh of 400-m nodes in the horizontal direction and 200 m in the vertical direction. In this case, the transmission frequency is 0.25 Hz for an x-directed dipole, the source is 50 m above the seafloor, the receiver is 1 m above the seafloor, and the source–receiver offset is 4000 m. We have computed the horizontal electric and magnetic field amplitude ratios (top two panels) and phase differences (bottom two panels) when an individual block is perturbed by making it 100 Ωm. We have plotted vertical slices through the array (second and fourth panels) and horizontal slices 200 m below the seafloor (first and third panels). The black contours outline where the amplitude ratios are plus or minus one part in 1000 (i.e., 0.1%) or the phase differences are ± 0.025°, showing that, effectively, the data are not sensitive to any structure deeper than or offset by more than about half the source–receiver spacing, or 2 km in this case.

ANISOTROPY

Marine sediments are almost always anisotropic to some extent, from the grain and fabric scale to interbedded layers of differing lithology, with the horizontal direction (along the fabric and bedding) being more conductive than the vertical direction (across the fabric and bedding). In addition, stacked reservoirs or reservoirs with interbedded shales will exhibit significant anisotropy. The marine CSEM community variously ignores anisotropy or declares it to be all-important (for examples of the latter, see Jing et al., 2008; and Lovatini et al., 2009). In the context of the previous section, this turns out to be correlated with the use of 1D/2D inversion and interpretation or 3D inversion and interpretation. Referring again to Figure 6, the radial fields might be expected to be sensitive to the vertical resistivity, and the azimuthal fields sensitive to the horizontal conductivity. This is indeed the case to a good approximation.

In Figure 12, we have computed fields over three 1D models (all in 1000-m seawater) using the DIPOLE1D code of Key (2009). Two models have an isotropic seafloor of either 1 Ωm or 0.51 Ωm, and a third model has been made anisotropic by alternating 50-m-thick layers of 1.7 Ωm and 0.3 Ωm, producing an anisotropy ratio of 2 with vertical and horizontal resistivity the same as for the two isotropic values. For radial fields, the anisotropic model produces almost identical responses to the 1-Ωm model (i.e., the vertical resistivity) for all three components. For the azimuthal fields, the anisotropic model produces a horizontal electric field and vertical magnetic field that are almost identical to the 0.51-Ωm horizontal resistivity. We have not plotted phase, but it behaves similarly. The horizontal magnetic field in the azimuthal direction is the only component that does not behave simply, but this component is going through a phase reversal associated with the interaction of the airwave with the seafloor fields.

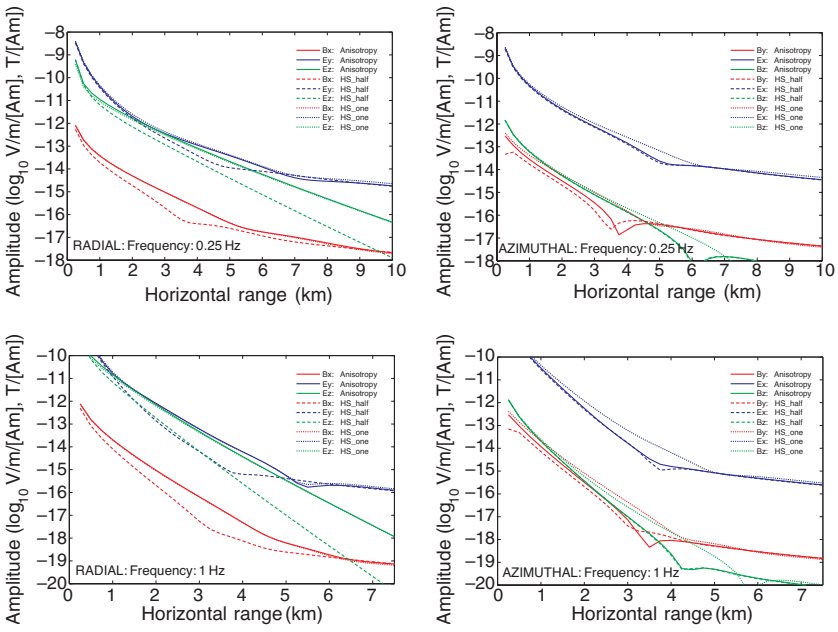

Figure 12. Radial (left panels) and azimuthal (right panels) electric (blue) and magnetic (red) field amplitudes as a function of source–receiver offset over a half-space in 1000-m water depth (radial Ez and azimuthal Bz are both shown in green). Three half-space (HS) resistivities are considered, 1 Ωm (dotted lines), 0.51 Ωm (broken lines), and an anisotropic half-space with 1 Ωm in the vertical direction and 0.51 Ωm in the two horizontal directions ("Anisotropy," solid lines). The top panels show responses at 0.25 Hz, and the bottom panels show 1-Hz fields. For radial fields, the anisotropic model produces very similar responses to the 1-Ωm model (i.e., the vertical resistivity) for all three components. For the azimuthal fields, the anisotropic model produces a horizontal electric field and a vertical magnetic field that is very similar to the 0.51-Ωm horizontal resistivity. The phase (not shown here) behaves similarly.

Thus, for imaging oil and gas reservoirs, characterized by their vertical resistivity-thickness product, inverting amplitude and phase of the radial (inline) components is likely to provide a good result in terms of depth and transverse resistance of the target (just as Key, 2009, showed). The sediment resistivity will be mostly correct as well, so long as one is aware that it is the vertical resistivity that is being imaged. For imaging reservoirs, one does not use azimuthal field data on their own (because they are poorly sensitive to thin horizontal resistors), but instead in combination with radial field data, as is typically done for 3D interpretations. In that case, any significant anisotropy is going to make it impossible to model both modes with a common isotropic resistivity, even if the modeling is done in three dimensions. In other words, when modeling radial data in one or two dimensions, what you do not know does not hurt you, but for modeling inline and off-line data in three dimensions, anisotropy will usually have to be included.

There will be limits, however, in the ability to ignore anisotropy when interpreting radial mode data. In the example presented here, the differences between the anisotropic and isotropic radial fields are as large as 20%. This might be accommodated when inverting one component and one frequency, but could prove problematic when inverting multicomponent and/or multifrequency data. For example, the horizontal electric field in the range between 2 and 5 km at 1 Hz is within about 2% of the anisotropic response, whereas at the frequency of 0.25 Hz the responses are from 10% to 20% different. The phase differences are about 10° at both frequencies, consistent with the 15% amplitude difference. However, whereas the field magnitudes for the anisotropic model are smaller than for the isotropic model, the phase lags are also smaller. This is exactly the opposite behavior than seen for isotropic models — normally, decreasing seafloor resistivity decreases the size of the fields and increases the size of the phase lag.

Thus, isotropic inversion of radial data from an anisotropic seafloor is likely to produce bias between simultaneous fits to amplitude and phase. As we discuss below, navigation errors probably limit the accuracy of typical CSEM data to about 10%, so the effects we discuss here might not be significant, but as we collect better data they will become so. For example, Myer et al. (2010) observe a bias in amplitude and phase fits when inverting multifrequency radial electric field data with a 2% error floor.

THE SHALLOW-WATER PROBLEM AND TIME DOMAIN

The marine CSEM method was conceived as a way to take advantage of EM propagation in the deepwater, resistive-seafloor environment (Cox, 1981). Skin depths in seawater at typical CSEM frequencies (from 0.1 to 10 Hz) are less than a kilometer and, more typically, only a few hundred

meters. In the igneous seafloor rocks of the deep ocean, corresponding skin depths are tens of kilometers or more. This ensures that for seafloor transmitters and receivers separated by many seawater skin depths, energy propagates almost entirely through the earth, with no "primary" response from the transmitter, and it provides exceptional sensitivity to the seafloor conductivity structure. Even over the more conductive rocks of sedimentary basins on the continental shelf, this effect holds for water depths of about a kilometer and source–receiver ranges as much as about 5 to 10 km, making CSEM an effective method for exploring several kilometers into the earth.

At greater ranges, energy that has leaked into the atmosphere above the transmitter and propagates back down to the seafloor begins to dominate the CSEM signal. This "airwave" is a consequence of the lack of attenuation in the atmosphere, with only geometric spreading reducing the signal strength with distance. This can be seen in the slight inflection followed by shallowing of the horizontal fields in Figure 12, and (as noted above) is responsible for more complicated behavior in the azimuthal magnetic fields.

Indeed, careful inspection of Figure 12 shows that the difference between anisotropic and isotropic responses is greatest at the onset of the airwave for all horizontal components. In addition, the difference between the isotropic and anisotropic responses significantly changes size once the airwave becomes more dominant, the difference getting larger for the radial field and smaller for the azimuthal fields. For example, the 1-Hz horizontal electric field in the radial direction goes from being about 2% different at shorter ranges to 17% different at longer ranges, whereas the azimuthal field goes from being more than 15% different to about 3%. The azimuthal magnetic field is most dramatic, going from 100% different to about 1% different. The explanation is simple; the energy propagating down from the atmosphere is essentially horizontal, and so will couple to the horizontal conductivity in the anisotropic model. For the azimuthal fields, wherein the isotropic model follows the horizontal conductivity, the approximation only gets better. For the radial fields, sensitive to the vertical resistivity, the approximation gets worse once the airwave dominates.

Many exploration targets lie in relatively shallow water (about 50 to 300 m in this context), where the advantage of the deepwater CSEM method is diminished by the dominance of the airwave signal. This has led to the development of schemes to remove the airwave signal from seafloor CSEM data (e.g., Amundsen et al., 2006). These removal methods require an estimate of seafloor conductivity and data of sufficient quality and spatial extent to carry out a transformation to the frequency-wavenumber domain. The main purpose of airwave removal seems to be to improve the signal in normalized responses, and the method presumably holds no advantage if the data are being modeled or inverted using code that includes the air layer.

Indeed, as papers by Nordskag and Amundsen (2007) and Andréis and MacGregor (2008) show, the airwave is coupled to seafloor conductivity and contains information about seafloor structure, and one should remember that frequency-domain EM methods have been used on land in spite of the primary signal in the atmosphere (e.g., the Turam method). The critical aspect of working in shallower water is that the signal from the target becomes a smaller part of the total signal, and the only way to compensate for that is by collecting higher quality data and correctly modeling the airwave component, either explicitly or by a transformation.

Experience from land EM suggests that the best approach to dealing with the airwave is by using time-domain (TEM), instead of frequency-domain, methods (e.g., Weiss, 2007). Figure 13, from Li and Constable (2010), illustrates this method by plotting the horizontal electric field TEM responses over a shallow 1D reservoir in 100-m water depth, with the half-space responses plotted for comparison. The impulse response shows a peak at about 0.01 s, which is the airwave arrival, and then a second peak about 0.3 to 0.6 s associated with the target reservoir.

Impulse responses are favored by TEM practitioners because they show the airwave separation at early time and look somewhat similar to seismic traces, but the step-on response shows the data that would actually be collected. The effect of the reservoir is still clearly seen, but the signal strengths are now evident. This is important, because the traditional disadvantage of the TEM method over frequency-domain methods is a smaller signal-to-noise ratio (S/N). The lower S/N results from the spreading of energy across the entire spectrum and the need for long recording windows, here 100 s before the signal asymptotically approaches steady state at the 6-km offset. Frequency-domain noise floors at 1 Hz with about 100-s stacking are typically about 10^{-15} V/(Am^2), so loss of stacking alone raises this value an order of magnitude. A greater problem is that noise associated with water motion and magnetotelluric signals increases with period and is also greater in shallow water, so although the signals shown in Figure 13 are probably measurable, the S/N would not be very high. The considerable stacking times required by TEM data collection have required stationary transmitters in the past, considerably increasing the cost of marine data acquisition.

In the case shown in Figure 13, the receivers are on the seafloor and the transmitter is in midwater, 50 m below the surface, but modeling shows that sensitivity to the target does not change greatly with the placement of transmitter and receivers in the water column. This suggests a surface-towed system of transmitters and receivers, allowing simpler equipment and faster towing speeds than deepwater CSEM methods using deployed receivers and deep-towed transmitters. Indeed, both the industry and our group have started experimenting with towed arrays, but our experience is that the noise and

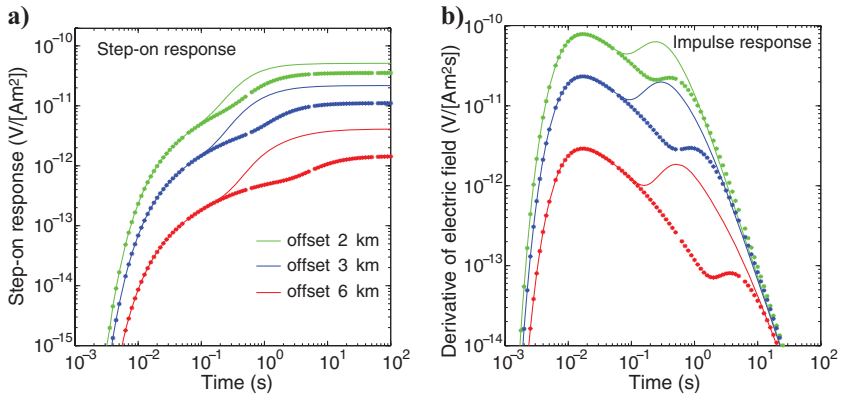

Figure 13. Step-on and impulse horizontal electric field response at seafloor receivers excited by a horizontal electric dipole transmitter positioned 50 m above the seafloor in water 100 m deep. A 100-m thick, 100-Ωm reservoir is buried 500 m deep in a 1-Ωm half-space. The reservoir response (solid lines) is distinct from the half-space response (symbols) after 0.1 to 0.5 s. Modified from Li and Constable (2010).

stacking problems described above are worse when towing a receiver at the surface.

Finally, by plotting the step-on response, one can see the signature of the target reservoir in the late time response, characteristic of the DC resistivity method (known to be sensitive to thin resistive layers). As one might expect, by going to long-enough periods the frequency-domain method also starts to approximate the DC method and can detect this relatively large and shallow reservoir in spite of the air. A 10-s period appears to approximate DC in this case (Figure 14), at which point phase shifts are only about 25°, and the difference in amplitude with and without the target is about half that of the DC limit. Although lowering the frequency helps to combat the airwave problem, the response is much smaller than for deepwater CSEM sounding, and the reader is reminded of the lack of intrinsic depth resolution in the DC resistivity method. Interestingly, the phase response of the target is appreciable at 1 Hz, even though the amplitude response at this frequency is small, a phenomenon noted by Mittet (2008), who shows that in shallow water the CSEM phase might be more diagnostic of the reservoir response than amplitude.

EQUIPMENT AND NAVIGATION ERRORS

Significant improvements have been made in transmitter and receiver reliability over the last 10 years, and the noise floor of the transmitter-receiver system has also become significantly better through a combination of an order of magnitude increase in the source dipole moment and a similar decrease in the receiver noise floor compared with the earliest academic equipment. In other respects, the equipment used for marine CSEM has not changed much since the start of commercial operations. Efforts toward new instrument systems seem to be focused on continuously towed receivers, which might improve data collection efficiency and drive costs down but are unlikely to improve signal-to-noise ratios, resolution, or depth of investigation. As noted by Constable and Srnka (2007), it is unlikely that present transmitter currents of about 1000 amps will increase significantly, given the limitations represented by conductivities of seawater and copper, and at some point environmental concerns will become an issue with large transmitter moments. More likely, receiver sensitivity can be made better — present instruments are still about an order of magnitude noisier than the thermal noise limits of the electrode circuit.

One of the main limitations on CSEM data quality at this time appears to be the navigation of the transmitter. Figure 15 illustrates how errors in the source–receiver range propagate into CSEM data at 0.75 Hz. Higher frequencies have steeper amplitude-versus-offset curves and thus a larger propagation of range errors into data errors. To a first approximation, a fractional CSEM error given a range error of δ for skin depth in the seafloor of z_s goes at δ / z_s. Thus a 10-m error at 1 Hz over 1-Ωm sediment gives an error of about 2%. At short ranges where skin depth in seawater is most relevant, errors are about 4%.

Short baseline (SBL) acoustic systems, whereby the range and direction of a transponder mounted on the transmitter is obtained from transceivers on the survey vessel, represent the most popular approach to transmitter navigation. The vessel position and orientation are obtained using the global positioning system (GPS) and a motion reference unit (MRU). The SBL systems have advertised accuracies of about 0.25% in range and about 0.25° in angle, and thus under ideal operating conditions one might expect range errors of no worse than 8 m and cross-range errors of no worse than 13 m for a position estimate from a single vessel location at a slant range of 3000 m. In practice, position errors could approach 50 m because of either poor calibration or bad weather, and ultimately these systems are limited to operating depths of a few kilometers.

As the quantitative interpretation of marine CSEM data improves, greater effort will need to be put into the navigation of the transmitter to drive the systematic errors down toward a few percent. Receiver navigation might also be an issue with some data sets, but that is something that does not require any significant improvement in terms of current technology because external recording compasses provide reasonable orientations and, unlike the transmitter, it is pos-

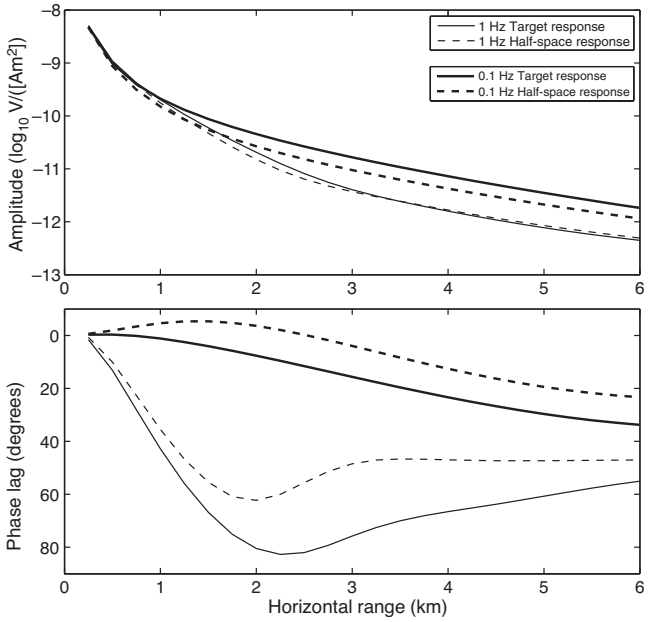

Figure 14. The frequency-domain response of model and transmitter/receiver combinations shown in Figure 13, for 0.1 and 1 Hz. A significant phase response occurs at 1 Hz and a significant amplitude response at 0.1 Hz.

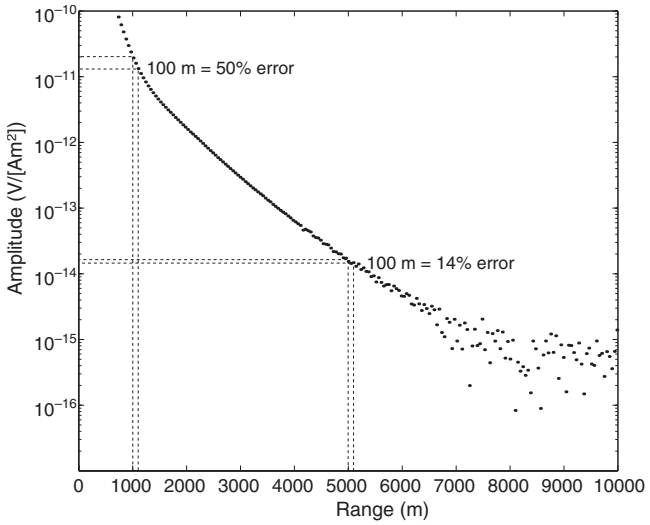

Figure 15. The effect of a 100-m error in the source-receiver range on the quality of 0.75-Hz CSEM data. The errors would be worse at higher frequencies.

sible to collect redundant SBL or long baseline (LBL) data when the target is not itself in motion.

OTHER APPLICATIONS OF MARINE CSEM

Although most marine CSEM activity to date has been carried out for exploration and predrill appraisal, it has been obvious for some time that there could be an application in monitoring the production of reservoirs, and two recent papers present model studies to examine this (Lien and Mannseth, 2008; Orange et al., 2009). If the reservoir is large enough to generate a CSEM signal before production, then one can expect changes to occur in the CSEM response as a result of any change in the size and shape of the reservoir. Because the total production is known, and the horizons at which the changes can occur are also constrained, resolution will be better than for the exploration case because there will be no trade-off between the resistivity signature of the reservoir and that of the host rocks. Indeed, it could be that the host-rock resistivity structure does not need to be known in detail because it will not change with time. As in seismic time-lapse studies, accurate repositioning of receivers or permanent installation might be necessary, although the diffusion equation could be more forgiving than the wave equation in this case. Nevertheless, Orange et al. (2009) show that data need to be repeatable to about 1% to generate meaningful differences in CSEM responses.

Another application of marine CSEM is likely to be the exploration for gas hydrates as a methane resource, and possibly predrill surveys to mitigate hazard represented by hydrates and shallow gas. First proposed by Edwards (1997), the use of marine EM to study seafloor gas hydrate is gaining traction (Yuan and Edwards, 2000; Schwalenberg et al., 2005; Weitemeyer et al., 2006; Darnet et al., 2007; Evans, 2007; Ellis et al., 2008; Zach and Brauti, 2009; Schwalenberg et al., 2010). One of the driving forces behind this trend is that it is difficult to quantify the concentration of hydrate in the sedimentary section using seismics alone. The existence of a bottom-simulating reflector (BSR), the marked seismic response to traces of free gas at the edge of the hydrate stability field, has proved to be largely uncorrelated with the presence of hydrate in the section above. The CSEM equipment adapted to the study of the shallow parts of the section is also likely to be used in the search for, and study of, offshore fresh-groundwater resources.

CONCLUSIONS

At the age of 10 years, commercial marine CSEM has been through the boom and bust of overly enthusiastic early adoption (or overselling, depending on one's perspective), and now appears to be on the path to long-term acceptance and integration into the exploration toolkit. It is clearly a useful tool for mapping seafloor resistivity but requires sophisticated modeling and inversion to turn raw data into interpretable resistivity estimates. Modeling and inversion codes are available, but little has been published in the way of comparisons using different algorithms and dimensionality. Because resistivity alone is not a definitive indicator of hydrocarbons, integration with other geologic and geophysical data sets is an essential next step after modeling, but overlaying resistivity images on seismic reflection profiles seems to be the extent of present practice. Several groups are working on more rigorous joint seismic and CSEM inversion, but the differing data densities, differing resolving power, and lack of unique rock physics relationships between seismic velocity and resistivity make this a challenging problem. The payoff, however, is likely great because the combination of the seismic method's resolution and the CSEM method's sensitivity to a critically important physical property will be much more powerful than the combination of seismic and potential-field data.

ACKNOWLEDGMENTS

The author thanks Rune Mittet, other reviewers, the editors, David Myer, and Arnold Orange for their helpful comments; Chet Weiss and Kerry Key for making their codes available; and the Seafloor Electromagnetic Methods Consortium at Scripps Institution of Oceanography for financial support. And special thanks go to Chip Cox, for inviting the author to join him as a postdoc to work in marine CSEM all those years ago.

REFERENCES

Abubakar, A., T. M. Habashy, V. L. Druskin, L. Knizhnerman, and D. Alumbaugh, 2008, 2.5D forward and inverse modeling for interpreting low frequency electromagnetic measurements: Geophysics, **73**, no. 4, F165–F177, doi: 10.1190/1.2937466.

Amundsen, L., L. Løseth, R. Mittet, S. Ellingsrud, and B. Ursin, 2006, Decomposition of electromagnetic fields into upgoing and downgoing components: Geophysics, **71**, no. 5, G211–G223, doi: 10.1190/1.2245468.

Andréis, D., and L. MacGregor, 2008, Controlled-source electromagnetic sounding in shallow water: Principles and applications: Geophysics, **73**, no. 1, F21–F32, doi: 10.1190/1.2815721.

Baba, K., 2005, Electrical structure in marine tectonic settings: Surveys in Geophysics, **26**, 701–731, doi: 10.1007/s10712-005-1831-2.

Bannister, P. R., 1968, Determination of the electrical conductivity of the sea bed in shallow waters: Geophysics, **33**, 995–1003, doi: 10.1190/1.1439993.

Belash, V. A., 1981, Characteristic features of undersea electromagnetic sounding: Geophysical Journal, **3**, 860–875.

Brock-Nannestad, L., 1965, Determination of the electrical conductivity of the seabed in shallow waters with varying conductivity profile: Electronics Letters, **1**, no. 10, 274–276, doi: 10.1049/el:19650249.

Cagniard, L., 1953, Basic theory of the magnetotelluric method of geophysical prospecting: Geophysics, **18**, 605–635, doi: 10.1190/1.1437915.

Carazzone, J. J., T. A. Dickens, K. E. Green, C. Jing, L. A. Wahrmund, D. E. Willen, M. Commer, and G. A. Newman, 2008, Inversion study of a large marine CSEM survey: 78th Annual International Meeting, SEG, Expanded Abstracts, 644–647.

Chave, A. D., S. C. Constable, and R. N. Edwards, 1991, Electrical exploration methods for the seafloor, *in* M. Nabighian, ed., Electromagnetic methods in applied geophysics, vol. 2: SEG Investigations in Geophysics No. 3, 931–966.

Chave, A. D., and C. S. Cox, 1982, Controlled electromagnetic sources for measuring electrical conductivity beneath the oceans: Part 1 — Forward problem and model study: Journal of Geophysical Research, **87**, B7 5327–5338, doi: 10.1029/JB087iB07p05327.

Cheesman, S. J., R. N. Edwards, and A. D. Chave, 1987, On the theory of seafloor conductivity mapping using transient electromagnetic systems: Geophysics, **52**, 204–217, doi: 10.1190/1.1442296.

Coggon, J. H., and H. F. Morrison, 1970, Electromagnetic investigation of the sea floor: Geophysics, **35**, 476–489, doi: 10.1190/1.1440109.

Commer, M., and G. A. Newman, 2008, New advances in three-dimensional controlled-source electromagnetic inversion: Geophysical Journal International, **172**, no. 2, 513–535, doi: 10.1111/j.1365-246X.2007.03663.x.

Commer, M., G. A. Newman, J. J. Carazzone, T. A. Dickens, K. E. Green, L. A. Wahrmund, D. E. Willen, and J. Shiu, 2008, Massively parallel electrical-conductivity imaging of hydrocarbons using the IBM Blue Gene/L supercomputer: IBM Journal of Research and Development, **52**, no. 1, 93–103, doi: 10.1147/rd.521.0093.

Constable, S. C., 1990, Marine electromagnetic induction studies: Surveys in Geophysics, **11**, no. 2–3, 303–327, doi: 10.1007/BF01901663.

Constable, S., and C. S. Cox, 1996, Marine controlled source electromagnetic sounding 2: The PEGASUS experiment: Journal of Geophysical Research, **101**, B3 5519–5530, doi: 10.1029/95JB03738.

Constable, S. C., C. S. Cox, and A. D. Chave, 1986, Offshore electromagnetic surveying techniques: 56th Annual International Meeting, SEG, Expanded Abstracts, 81–82, doi: 10.1190/1.1892948.

Constable, S., K. Key, and D. Myer, 2009, Marine electromagnetic survey of Scarborough gas field, preliminary cruise report, http://marineemlab.ucsd.edu/Projects/Scarborough/, accessed 21 May 2010.

Constable, S., A. Orange, G. M. Hoversten, and H. F. Morrison, 1998, Marine magnetotellurics for petroleum exploration: Part 1 — A sea-floor equipment system: Geophysics, **63**, 816–825, doi: 10.1190/1.1444393.
Constable, S. C., R. L. Parker, and C. G. Constable, 1987, Occam's inversion: A practical algorithm for generating smooth models from electromagnetic sounding data: Geophysics, **52**, 289–300, doi: 10.1190/1.1442303.
Constable, S., and L. J. Srnka, 2007, An introduction to marine controlled source electromagnetic methods for hydrocarbon exploration: Geophysics, **72**, no. 2, WA3–WA12, doi: 10.1190/1.2432483.
Constable, S., and C. J. Weiss, 2006, Mapping thin resistors and hydrocarbons with marine EM methods: Insights from 1D modeling: Geophysics, **71**, no. 2, G43–G51, doi: 10.1190/1.2187748.
Cox, C. S., 1980, Electromagnetic induction in the oceans and inferences on the constitution of the earth: Geophysical Surveys, **4**, no. 1–2, 137–156, doi: 10.1007/BF01452963.
Cox, C. S., 1981, On the electrical conductivity of the oceanic lithosphere: Physics of the Earth and Planetary Interiors, **25**, no. 3, 196–201, doi: 10.1016/0031-9201(81)90061-3.
Cox, C. S., A. D. Chave, and S. Constable, 1984, Offshore controlled source EM surveying, University of California proposal, http://marineem.ucsd.edu/pubs.html, accessed 27 July 2010.
Cox, C. S., S. C. Constable, A. D. Chave, and S. C. Webb, 1986, Controlled source electromagnetic sounding of the oceanic lithosphere: Nature, **320**, no. 6057, 52–54, doi: 10.1038/320052a0.
Cox, C. S., T. K. Deaton, and P. Pistek, 1981, An active source EM method for the seafloor, Scripps Institution of Oceanography technical report, http://escholarship.org/uc/item/7dr96489, accessed 25 May 2010.
Cox, C. S., J. H. Filloux, and J. C. Larsen, 1971. Electromagnetic studies of ocean currents and electrical conductivity below the ocean floor, *in* A. E. Maxwell, ed., The sea, vol. 4: Wiley, 637–693.
Darnet, M., M. C. K. Choo, R. Plessix, M. L. Rosenquist, K. Yip-Cheong, E. Sims, and J. W. K. Voon, 2007, Detecting hydrocarbon reservoirs from CSEM data in complex settings: Application to deepwater Sabah, Malaysia: Geophysics, **72**, no. 2, WA97–WA103.
Edwards, R. N., 1997, On the resource evaluation of marine gas hydrate deposits using sea-floor transient electric dipole-dipole methods: Geophysics, **62**, 63–74, doi: 10.1190/1.1444146.
Edwards, R. N., and A. D. Chave, 1986, A transient electric dipole-dipole method for mapping the conductivity of the sea floor: Geophysics, **51**, 984–987, doi: 10.1190/1.1442156.
Edwards, R. N., L. K. Law, P. A. Wolfgram, D. C. Nobes, M. N. Bone, D. F. Trigg, and J. M. DeLaurier, 1985, First results of the MOSES experiment: Sea sediment conductivity and thickness determination, Bute Inlet, British Columbia, by magnetometric offshore electrical sounding: Geophysics, **50**, 153–161, doi: 10.1190/1.1441825.
Edwards, R. N., D. C. Nobes, and E. Gómez-Treviño, 1984, Offshore electrical exploration of sedimentary basins: The effects of anisotropy in horizontally isotropic, layered media: Geophysics, **49**, 566–576, doi: 10.1190/1.1441691.
Eidesmo, T., S. Ellingsrud, L. M. MacGregor, S. Constable, M. C. Sinha, S. Johanson, F. N. Kong, and H. Westerdahl, 2002, Sea bed logging (SBL), a new method for remote and direct identification of hydrocarbon filled layers in deepwater areas: First Break, **20**, 144–152.
Ellingsrud, S., T. Eidesmo, S. Johansen, M. C. Sinha, L. M. MacGregor, and S. Constable, 2002, Remote sensing of hydrocarbon layers by seabed logging (SBL): Results from a cruise offshore Angola: The Leading Edge, **21**, 972–982, doi: 10.1190/1.1518433.
Ellis, M., R. Evans, D. Hutchinson, P. Hart, J. Gardner, and R. Hagen, 2008, Electromagnetic surveying of seafloor mounds in the northern Gulf of Mexico: Marine and Petroleum Geology, **25**, no. 9, 960–968, doi: 10.1016/j.marpetgeo.2007.12.006.
Evans, R. L., 2007, Using CSEM techniques to map the shallow section of seafloor: From the coastline to the edges of the continental slope: Geophysics, **72**, no. 2, WA105–WA116, doi: 10.1190/1.2434798.
Filloux, J. H., 1967a, An ocean bottom, *D* component magnetometer: Geophysics, **32**, 978–987, doi: 10.1190/1.1439910.
Filloux, J. H., 1967b, Oceanic electric currents, geomagnetic variations and the deep electrical conductivity structure of the ocean-continents transition of central California: Ph.D. thesis, University of California San Diego.
Filloux, J. H., 1973, Techniques and instrumentation for study of natural electromagnetic induction at sea: Physics of the Earth and Planetary Interiors, **7**, no. 3, 323–338, doi: 10.1016/0031-9201(73)90058-7.
Filloux, J. H., 1974, Electric field recording on the sea floor with short span instruments: Journal of Geomagnetism and Geoelectricity, **26**, 269–279.
Flosadóttir, A. H., and S. Constable, 1996, Marine controlled source electromagnetic sounding 1: Modeling and experimental design: Journal of Geophysical Research, **101**, B3, 5507–5517, doi: 10.1029/95JB03739.
Fonarev, G. A., 1982, Electromagnetic research in the ocean: Geophysical Surveys, **4**, no. 4, 501–508, doi: 10.1007/BF01449113.
Hoversten, G. H., S. Constable, and H. F. Morrison, 2000, Marine magnetellurics for base salt mapping: Gulf of Mexico field-test at the Gemini structure: Geophysics, **65**, 1476–1488, doi: 10.1190/1.1444836.
Hoversten, G. M., H. F. Morrison, and S. Constable, 1998, Marine magnetotellurics for petroleum exploration: Part 2 — Numerical analysis of subsalt resolution: Geophysics, **63**, 826–840, doi: 10.1190/1.1444394.
Jing, C., K. Green, and D. Willen, 2008, CSEM inversion: Impact of anisotropy, data coverage, and initial models: 78th Annual International Meeting, SEG, Expanded Abstracts, 604–608, doi: 10.1190/1.3063724.
Key, K., 2009, 1D inversion of multicomponent, multifrequency marine CSEM data: Methodology and synthetic studies for resolving thin resistive layers: Geophysics, **74**, no. 2, F9–F20, doi: 10.1190/1.3058434.
Key, K. W., S. C. Constable, and C. J. Weiss, 2006, Mapping 3D salt using the 2D marine magnetelluric method: Case study from Gemini Prospect, Gulf of Mexico: Geophysics, **71**, no. 1, B17–B27, doi: 10.1190/1.2168007.
Lee, M. W., 2004, Elastic velocities of partially gas-saturated unconsolidated sediments: Marine and Petroleum Geology, **21**, no. 6, 641–650, doi: 10.1016/j.marpetgeo.2003.12.004.
Li, Y., and K. Key, 2007, 2D marine controlled-source electromagnetic modeling: Part 1 — An adaptive finite-element algorithm: Geophysics, **72**, no. 2, WA51–WA62, doi: 10.1190/1.2432262.
Li, Y. G., and S. Constable, 2010, Transient electromagnetic in shallow water: insights from 1D modeling: Chinese Journal of Geophysics, **53**, 737–742.
Lien, M., and T. Mannseth, 2008, Sensitivity study of marine CSEM data for reservoir production monitoring: Geophysics, **73**, no. 4, F151–F163, doi: 10.1190/1.2938512.
Løseth, L. O., H. M. Pedersen, B. Ursin, L. Amundsen, and S. Ellingsrud, 2006, Low-frequency electromagnetic fields in applied geophysics: Waves or diffusion?: Geophysics, **71**, no. 4, W29–W40, doi: 10.1190/1.2208275.
Løseth, L. O., and B. Ursin, 2007, Electromagnetic fields in planarly layered anisotropic media: Geophysical Journal International, **170**, no. 1, 44–80, doi: 10.1111/j.1365-246X.2007.03390.x.
Lovatini, A., M. D. Watts, K. E. Umbach, A. Ferster, S. Patmore, and J. Stilling, 2009, Application of 3D anisotropic CSEM inversion offshore west of Greenland: 79th Annual International Meeting SEG, Expanded Abstracts, 830–834.
MacGregor, L., M. Sinha, and S. Constable, 2001, Electrical resistivity structure of the Valu Fa Ridge, Lau Basin, from marine controlled-source electromagnetic sounding: Geophysical Journal International, **146**, no. 1, 217–236, doi: 10.1046/j.1365-246X.2001.00440.x.
Minerals Management Service, 2010, Data accessed 27 May 2010 at http://www.gomr.mms.gov/homepg/fastfacts/WaterDepth/wdmaster.asp.
Mittet, R., 2008, Normalized amplitude ratios for frequency-domain CSEM in very shallow water: First Break, **26**, 47–54.
Mittet, R., and T. Schaug-Pettersen, 2008, Shaping optimal transmitter waveforms for marine CSEM surveys: Geophysics, **73**, no. 3, F97–F104, doi: 10.1190/1.2898410.
Myer, D., S. Constable, and K. Key, 2010, A marine EM survey of the Scarborough gas field: Northwest Shelf of Australia: First Break, **28**, 77–82.
Newman, G. A., and D. L. Alumbaugh, 1997, Three-dimensional massively parallel electromagnetic inversion: Part 1 — Theory: Geophysical Journal International, **128**, no. 2, 345–354, doi: 10.1111/j.1365-246X.1997.tb01559.x.
Nordskag, J. I., and L. Amundsen, 2007, Asymptotic airwave modeling for marine controlled-source electromagnetic surveying: Geophysics, **72**, no. 6, F249–F255, doi: 10.1190/1.2786025.
Orange, A., K. Key, and S. Constable, 2009, The feasibility of reservoir monitoring using time-lapse marine CSEM: Geophysics, **74**, no. 2, F21–F29, doi: 10.1190/1.3059600.
Palshin, N. A., 1996, Oceanic electromagnetic studies: A review: Surveys in Geophysics, **17**, no. 4, 455–491, doi: 10.1007/BF01901641.
Price, A., P. Turpin, M. Erbetta, D. Watts, and G. Cairns, 2008, 1D, 2D, and 3D modeling and inversion of 3D CSEM data offshore West Africa: 78th Annual International Meeting, SEG, Expanded Abstracts, 639–643.
Schwalenberg, K., E. Willoughby, R. Mir, and R. N. Edwards, 2005, Marine gas hydrate electromagnetic signatures in Cascadia and their correlation with seismic blank zones: First Break, **23**, 57–63.
Schwalenberg, K., W. Wood, I. Pecher, L. Hamdan, S. Henrys, M. Jegen, and R. Coffin, 2010, Preliminary interpretation of electromagnetic, heat flow, seismic, and geochemical data for gas hydrate distribution across the Porangahau Ridge, New Zealand: Marine Geology, **272**, no. 1–4, 89–98, doi: 10.1016/j.margeo.2009.10.024.
Srnka, L. J., 1986, Method and apparatus for offshore electromagnetic sounding utilizing wavelength effects to determine optimum source and detector positions: U.S. Patent 4,617,518.
Trofimov, I. L., G. A. Fonarev, and V. S. Shneyer, 1973, Some results of magnetotelluric research in the central Arctic: Journal of Geophysical Research, **78**, no. 8, 1398–1400, doi: 10.1029/JB078i008p01398.
Unsworth, M., and D. Oldenburg, 1995, Subspace inversion of electromagnetic data: Application to mid-ocean-ridge exploration: Geophysical Journal International, **123**, no. 1, 161–168, doi: 10.1111/j.1365-246X.1995.tb06668.x.

Weiss, C. J., 2007, The fallacy of the "shallow-water problem" in marine CSEM exploration: Geophysics, **72**, no. 6, A93–A97, doi: 10.1190/1.2786868.

Weiss, C. J., and S. Constable, 2006, Mapping thin resistors and hydrocarbons with marine EM methods: Part 2 — Modeling and analysis in 3D: Geophysics, **71**, no. 6, G321–G332, doi: 10.1190/1.2356908.

Weitemeyer, K. A., S. C. Constable, K. W. Key, and J. P. Behrens, 2006, First results from a marine controlled-source electromagnetic survey to detect gas hydrates offshore Oregon: Geophysical Research Letters, **33**, no. 3, L03304, doi: 10.1029/2005GL024896.

Wolfgram, P. A., R. N. Edwards, L. K. Law, and M. N. Bone, 1986, Polymetallic sulfide exploration on the deep sea floor: The feasibility of the MINI-MOSES experiment: Geophysics, **51**, 1808–1818, doi: 10.1190/1.1442227.

Yuan, J., and R. N. Edwards, 2000, The assessment of marine gas hydrates through electronic remote sounding: Hydrate without a BSR?: Geophysical Research Letters, **27**, no. 16, 2397–2400, doi: 10.1029/2000GL011585.

Zach, J., and K. Brauti, 2009, Methane hydrates in controlled-source electromagnetic surveys — Analysis of a recent data example: Geophysical Prospecting, **57**, no. 4, 601–614, doi: 10.1111/j.1365-2478.2009.00809.x.